

Development of a UFAA-19 Series Hybrid Electric Vehicle

C.C. Kwasi-Effah^a, U.E. Igbeka^b, B.C. Ataman^c, A.I. Emenime^d, F. Max-Eguakun^e

^{a,b,c,d,e}Department of Mechanical Engineering, University of Benin, Ugbowo, Benin City, 300283, Nigeria

Article Info

Keywords:

Hybrid vehicle, emission, modelling
UFAA

Received 28 September 2021

Revised 15 November 2021

Accepted 28 November 2021

Available online 25 December 2021



<https://doi.org/10.37933/nipes/3.4.2021.35>

<https://nipesjournals.org.ng>

© 2021 NIPES Pub. All rights reserved

Abstract

Due to the ongoing control on emission levels and increase in fuel prices in many countries, it has become imperative for vehicle manufacturers to develop more fuel efficient drivetrain technologies. Hybrid electric vehicles are viewed as short- to mid-term solutions for reducing emissions and fuel consumption while maintaining vehicle performance. This paper presents a design of a UFAA-19 Series Hybrid Electric Vehicle to reduce the dependency on fossil fuels in Nigeria. A CAD model of the hybrid system was developed, afterwards, static and dynamic analyses were then carried out. Mild steel was the material used for the design and simulation of the model. The results from the static analysis showed that the model was stressed within permissible limits. The dynamic analysis showed that a 750W BLDC motor was sufficient for providing the low-speed torque for the mini hybrid system. The vehicle reached speeds of up to 17km/hr. Results also showed that an IC engine rated at 3.5kW would provide sufficient power for the system to reach up to speeds of 70km/hr. The hybridization factor for the system was found to be 17.6% which makes it a mild hybrid vehicle.

1. Introduction

With the introduction and widespread adoption of Nicolas Otto's Internal Combustion Engine for use in vehicles, air pollution from exhaust became a problem as harmful amounts of carbon monoxide and carbon dioxide were released into the atmosphere as well as smog [1]. In the world currently, 60% of CO emissions, 50% of NO emissions, and 30% of HC emissions are caused by automobiles [2]. To address the issue, automakers are being forced to shift a portion of their production from internal combustion engines to hybrid systems or pure electric vehicles. An electric vehicle that has zero fossil fuel by-products, also known as Zero-Emission Vehicles (ZEV), will provide a solution to this problem; however, the energy capacity and weights of electric batteries are still insufficient for replacements of internal combustion engines. The hybrid system is thus viewed as a suitable alternative.

Hybrid electric vehicles, HEVs, according to the International Electrotechnical Commission, are vehicles with propulsion energy from two or more sources, stores, or power converters and have at least one that's converted directly to electrical energy. Based on this definition, HEVs could be

classified based on their source of power as battery and gasoline ICE, battery and diesel ICE, battery and capacitors, and battery and flywheel [3]. This definition of HEVs is generally not accepted by ordinary people and as such a more suitable definition is required.

A hybrid vehicle combines more than one power source. It most commonly refers to vehicles that use both an internal combustion engine and an electrically powered motor, a Hybrid Electric Vehicle (HEV). HEVs can perform at least one of the following functions:

- engine idle start and stop
- energy recuperation (regenerative braking)
- electric torque assist
- electric driving
- battery charging (from the drive)
- battery charging (from the grid)

The emissions of Hybrid Electric Vehicles (HEVs) are generously less when contrasted with that of the Internal Combustion Engine Vehicles (ICEVs). Significant advantages of HEVs over ICEVs include better mileage, high efficiency, and improved productivity, less reliance on petroleum, reduced pollution because of the halfway or complete traction given by the electric motors.

The components providing a pathway for mechanical power in hybrid vehicles include the internal combustion engine, the transmission, the drivetrain, electric motors, and the alternator. For electrical power, we have the battery packs, the electric motors, the alternator, and the bidirectional power converter. Based on the arrangements of these components, HEVs can be classified into Series Hybrids, Parallel or Series-Parallel Hybrids, and Complex Hybrids (CHEV). [4].

Hybridization of an electric vehicle is the degree to which the vehicle's power is being assisted by a secondary power source such as an ICE. Hybridization factor is a measure of this power assist. It is represented as the ratio between the electric motor power and the sum of the total power input to the vehicle. It can be expressed mathematically as:

$$\text{Hybridization factor, } HF = \frac{\text{Motor power}}{\text{Motor power} + \text{Engine power}} \quad (1)$$

A summary of the different characteristics of the different classes of hybrid electric vehicles by hybridization degree is presented in Table 1.

Table 1: Comparison of different HEVs by the degree of hybridization

| Hybrid Type | Micro Hybrids | Mild Hybrids | Full Hybrids |
|----------------------|---------------|--------------|--------------|
| IC engine | Conventional | Downsized | Downsized |
| Motor power | 3 to 5kW | 7 to 15kW | 30 to 50kW |
| Motor voltage | 12V | 60 to 200V | 200 to 600V |
| Hybridization factor | < 10% | 10 to 30% | > 40% |
| Energy saving | 5 to 10% | 20 to 30% | 30 to 50% |

| | | | |
|----------------------|---|--|--|
| Functions | Idle start/stop Regenerative braking Accessory powering | Idle start/stop Regenerative braking Torque assist | Idle start/stop Regenerative braking Electric traction |
| Relative cost | Low | Medium | High |
| Example | Mercedes Smart | Honda Civic | Toyota Prius |

Modern HEVs use efficiency-enhancing technologies like regenerative braking where the vehicle's kinetic energy is converted to electric energy to charge batteries as opposed to heat energy as seen in conventional brakes. Many HEVs shut down the ICE at idle and at low speeds restarting it when necessary reducing idle emissions; this is called a start-stop system. Also, as HEVs have smaller engines than ICEVs the gear ratio can be adjusted for maximum efficiency to further improve economic fuel usage [5].

1.2 Vehicle Dynamics

The free-body diagram of a vehicle accelerating up an inclination is as shown in Figure 1. The diagram shows the vehicle accelerating with an instantaneous velocity, V , up a slope, θ , against a wind velocity, V_w . From Newton's second law of motion, the net force exerted on the vehicle is equal to the product of its mass and acceleration.

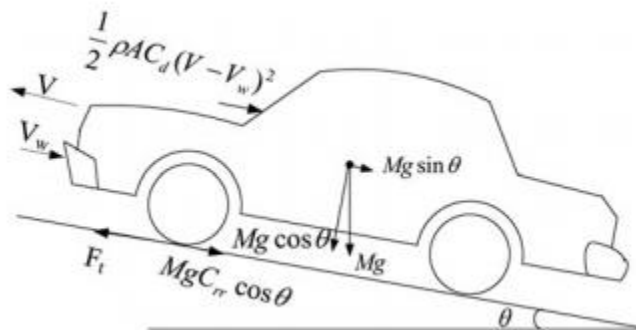


Figure 1: Free body diagram of a vehicle accelerating up an inclination

$$F_t - \sum F_r = f_m M \alpha$$

Where F_t = Traction force acting on the vehicle

$\sum F_r$ = Sum of all the resisting forces (drag, frictional and component of the vehicle's weight in its direction motion)

M = Overall mass of the vehicle

α = Acceleration of the vehicle

f_m = mass factor for converting the rotational mass of the rotating components into translating mass

$$\begin{aligned} \sum F_r &= F_D + F_f + Mg \sin \theta \\ &= \frac{1}{2} \rho A C_d (V - V_w)^2 + Mg C_{rr} \cos \theta + Mg \sin \theta \end{aligned}$$

Where A = Frontal area of the vehicle

ρ = Density of air

C_d = Drag coefficient

C_{rr} = Coefficient of rolling resistance

The total propulsion force is then given by

$$\Rightarrow \text{Traction force, } F_t = f_m M \quad (2)$$
$$\propto + \frac{1}{2} \rho A C_d (V - V_w)^2 + M g C_{rr} \cos \theta + M g \sin \theta$$

The power required to drive the vehicle at a speed, V , is given by the

$$\text{Power, } P = F_r \times V = f_m M \propto V + \frac{1}{2} \rho A C_d V (V - V_w)^2 + M g V C_{rr} \cos \theta + M g V \sin \theta$$

1.3 Literature Review

Balasubramani N. et al. designed and fabricated a two-wheeler hybrid electric system and studied its performance characteristics. The two-wheeler vehicle was powered in the front by an electric motor which was the hub motor and in the back by an IC engine. They tested the system in 3 modes; engine mode, electric mode, and hybrid mode, and compared the results with that gotten from a conventional two-wheeler system. They found out that the system gives twice the mileage as a conventional vehicle when the electric motor was used at start-up for generating high torque and the IC engine for sustaining the cruising speed. They also found out the hybrid system emitted 50% less pollution [6].

Grundit E. et al. modelled and simulated a series hybrid car, Smarter, using the MATLAB/Simulink graphical modelling software for competing in the 2009 Shell Eco-marathon competition. They varied the components of the drivetrain and investigated its effect on fuel efficiency. Although the model was never verified with a physical model, they found out that the car, Smarter, would cover 255km per litre of fuel and place 10th in the competition. They however discovered that further modification of the drivetrain parameters yielded little change in the vehicle's fuel efficiency and suggested that the parallel hybrid system be investigated [7].

Chuddy et al. carried out a study on the performance of a parallel and series hybrid system using a flexible Advanced Vehicle Simulator (ADVISOR). They studied the fuel economy of the two IC systems working independently and compared that with the savings from the parallel and series systems. The fuel economy was found to be 24% better than the IC engine running alone and 4% better than the series hybrid system [8].

Lukic et al. presented a study on the effect of hybridization on the fuel economy and dynamic performance of a vehicle. They studied the 3 different hybrid classes; micro, mild and full hybrid system for a conventional passenger vehicle. Their studies show that an acceptable level of fuel economy at a low price can be provided for by vehicles with a low hybridization factor. They also found out the optimum level of hybridization ranges between 30 to 50% and depends on the power requirement of the vehicle [9].

Kwasi-Effah et al. carried out a study on the fuel savings from a hybrid electric vehicle. They created a MATLAB/Simulink model of the hybrid system based off on the Toyota Prius series-

hybrid vehicle. The fuel consumption of the model was studied when it was subjected to the Urban Dynamometer Driving Schedule (UDDS) and the Highway Fuel Economy Test (HWFET) drive cycle data. They found out that the vehicular emission for the series-parallel system reduced by over 60% with emissions of 75g/km for CO₂, 0.096g/km for HC, 1.362g/km for CO, and 0.066g/km for NO_x [10, 11, 12].

Ceraolo M. et al. studied the problem of optimizing energy consumed by a hybrid system while considering two drivetrain configurations: the series and parallel drivetrains. For each configuration, the effect of the functions of different management strategies was considered (full electric drive, plug-in capabilities, etc.). They found out that the parallel hybrid system was superior to the series hybrid system [13, 14, 15].

2. Methodology

The model considered in this work was based on a go-kart. These are small open-wheeled suspension-less vehicles that are usually used for racing (karting). A conventional go-kart has 5 components: Chassis, steering system, power system, drivetrain, and braking system.

2.1 Conceptual Design

Vidyanandan, K V. [12] presented the different drivetrain configurations for hybrid vehicles. The concept chosen for this project was based off on the parallel hybrid drivetrain configuration. This configuration was chosen as opposed to the simpler series hybrid drivetrain because of the following reasons:

1. Compact design
2. High efficiency
3. Low cost
4. Low power requirements (i.e. smaller battery packs)

The low cost of the parallel hybrid drivetrain is due to the fewer number of components (when compared with the series-parallel and complex drivetrains) and their relatively small sizes (when compared with the series drivetrain). One of the reasons for this is due to the recycling of their motor for regenerative braking. We decided to capitalize on this and went with the conventional hybrid design as opposed to the plug-in hybrid design. Thus, we rely solely on regenerative braking to charge for batteries as well as the torque from the IC engine during the vehicle's cruising speed.

Since the target vehicle for this project is a go-kart, the rear-wheel-drive transmission system was chosen. Rear-wheel drive systems are favoured by racing cars of which a go-kart is one. As earlier stated, go-karts, aside from those used for recreational purposes, are usually designed for racing (karting).

In summary, the conceptual design we went with was that for a conventional parallel hybrid electric vehicle

2.2 Design Specification

We wanted to build a simple but practical model of the parallel hybrid go-kart with the following specifications

1. Lightweight for better mobility
2. Low power requirement
3. Low cost
4. Durable

We were looking at reaching speeds up to 70km/hr (19.4m/s) with the mass of the system (kart and driver) not exceeding 180kg.

2.2.1 Preliminary Analysis

In order to proceed with a detailed design of the system, a preliminary analysis is presented below which would serve as the minimum specification for the kart. This section aims to estimate the minimum power needed by the electric motor in order to propel the kart.

2.2.1.1 Assumptions

1. The effect of drag is neglected
2. The kart is assumed to move through still air
3. The body is assumed to be a point mass

2.2.1.2 Parameters

Vehicle mass (kart + driver), $M = 180\text{kg}$
Top speed for EM, $V = 15\text{km/hr}$ (4.12m/s)
Acceleration time, $t = 10\text{s}$
Maximum incline angle, $\theta = 2^\circ$
Working surface = concrete
Coefficient of rolling resistance, $C_{rr} = 0.01$

2.2.1.3 Calculations

From equation 1.2, neglecting air drag, the traction force is given by

$$F_t = M \alpha + MgC_{rr} \cos \theta + Mg \sin \theta$$

From the kinematic equations of motion,

$$\text{Acceleration, } \alpha = \frac{\Delta V}{t}$$

$$\therefore \text{Traction force, } F_t = M \left(\frac{V}{t} + gC_{rr} \cos \theta + g \sin \theta \right)$$

$$= 180 \left(\frac{4.12}{10} + 9.81 \times 0.01 \times \cos 2^\circ + 9.81 \times \sin 2^\circ \right)$$

$$\therefore \text{Traction force, } F_t = 154.3\text{N}$$

The power required to sustain this speed by the EM is given by

$$\text{Power, } P = F_t \times V$$

$$= 154.3 \times 4.12$$

$$\Rightarrow \text{Power required, } P = 643\text{W}$$

Therefore, the least rating for the electric motor should be **643W**. This also sets the limit of the value for the rating of the IC engine to be used for the mini hybrid system.

2.3 Detailed Design

The goal in this section is to present the processes and analysis carried out in creating the form representing the mini hybrid system. It also entails the details carried out in sizing some of the critical components of the system. A CAD model of the mini hybrid system was created in Solidworks 2018. Mathematical models representing some of the dynamic systems of the model were created and simulated in Simulink. Mild steel was chosen as the material for the design and analysis. This is due to its high strength, availability and low cost. The material properties of mild steel are shown in Appendix A1.

2.3.1 Design of Static Components

The static components of the go-kart design are the front and rear chassis. The type of chassis that we went with was the open chassis design. This is because this type of kart design offers the least drag due to its low frontal area. Also, it has a good combination of simplicity and strength. The kart design was based off on the fixed axle go kart plans from KartFab.com. The two parts of the chassis were connected by hinges.

The front chassis of the go-kart provides support for the driver, the front axle and the steering system. The rear chassis houses the propulsion system and the rear shaft. The kart chassis were separated into these two compartments in order to isolate the propulsion system, which is the most critical system, from the rest components of the kart.

The strength was the most important criterion considered during the design of the kart. Also, the system was designed so that the number of weld joints would be kept to a minimum. This is to reduce the site of stress concentrations.

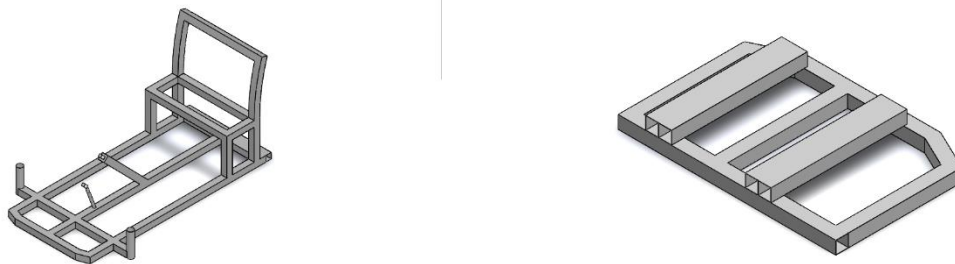


Figure 2: CAD model of front and rear chassis

2.3.2 Design of Dynamic Components

The dynamic components of the go-kart are the steering system and the electrical and IC propulsion systems.

2.3.2.1 Steering System

The Ackermann steering geometry was employed for the steering system. This was achieved with the help of a four-bar mechanical linkage consisting of a track rod, a tie rod, steering column and front axle. The steering column transfers the angular rotation of the steering to the pitman arm at its base. The tie rod forms a connection between the steering column and one of the front axles. It transmits the angular rotation of the steering column to the axle. The two front axles are connected by the track rod which enables the axles to rotate together.

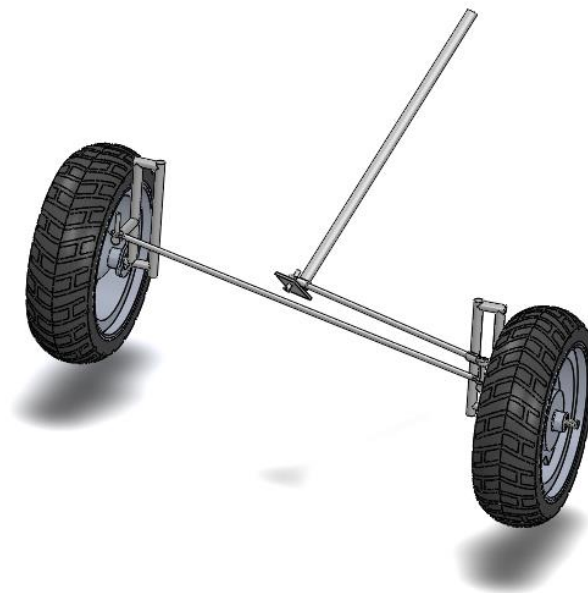


Figure 3: CAD model of the steering system

2.3.2.2 Electrical Propulsion System

From the results of the preliminary analysis, it can be seen that the rating of the electric motor should be greater than 643W. A 760W BLDC motor was selected for the hybrid system. In order to properly size the batteries, a simulation was carried out in the Simscape workspace of Matlab. The schematic for the model is as shown in Figure 4.

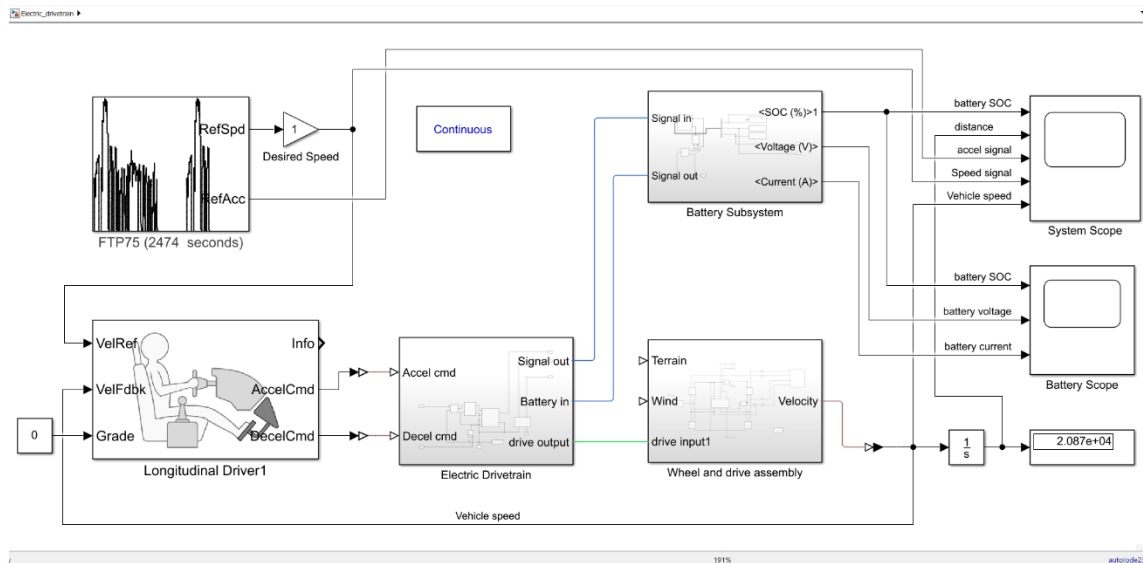
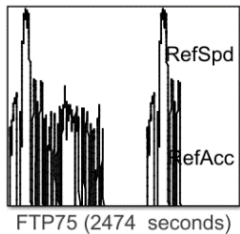


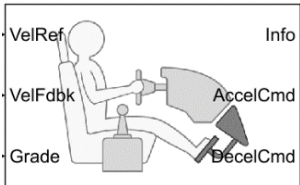
Figure 4: Model of the Vehicle showing the Electrical drivetrain

A breakdown of the different components of the model is presented as follows:



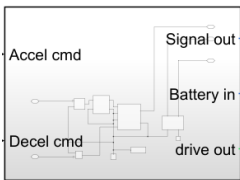
1. Drive Cycle:

This block generates a standard or user-specified longitudinal drive cycle. The block output is the vehicle longitudinal speed. This model makes use of the FTP75 drive cycle.



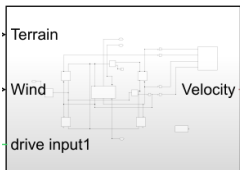
2. Longitudinal Driver:

This is a parametric longitudinal speed tracking controller for generating normalized acceleration and braking commands based on reference and feedback velocities.



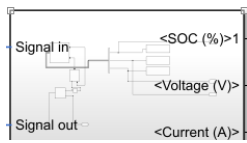
3. Electric Drivetrain:

This subsystem handles translating the acceleration and brake signals from the driver and translating that to mechanical torque signals to the vehicle.



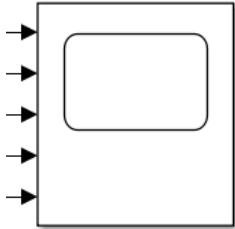
4. Wheel And Drive Assembly:

This contains the components that model the vehicle's body and the wheels.



5. Battery Subsystem:

This subsystem models the battery. Discharge, State of Charge, current and voltage values can be simulated with the input signal from the H-Bridge.



6. Scopes:

These are placed with the components to monitor the values and plot a graph of these against time. The scopes in this system monitor the vehicle's speed, distance travelled, and the battery's state of charge, voltage and current.

2.3.2.2 Working of the System

Reading off velocity values from the drive cycle input, the longitudinal driver sends either an acceleration signal or a brake signal to the drivetrain. This gets converted by the H-Bridge block to a Pulse-Width Modulated (PWM) voltage signal which is to be applied across the motor's terminals.

This output signal from the H-Bridge is first fed to the battery where the appropriate voltage, current and state of charge changes are applied. Then a lead from the battery supplies power to the DC Motor in the drivetrain.

The motor, once excited, applies a torque to the rear shaft of the vehicle through a chain drive (sprocket and chain) where a reduction ratio of 37:14 is applied. This torque on the shaft moves the rear wheels and the vehicle body. The velocity of the vehicle is measured and fed back to the longitudinal driver forming a closed-loop control system.

2.3.2.3 IC Propulsion System

Once the rating of the electric propulsion system was determined, an IC engine was selected based on vehicle rating proposed vehicle top speed. A Simulink model was created, and the ratings of the IC engine was varied.

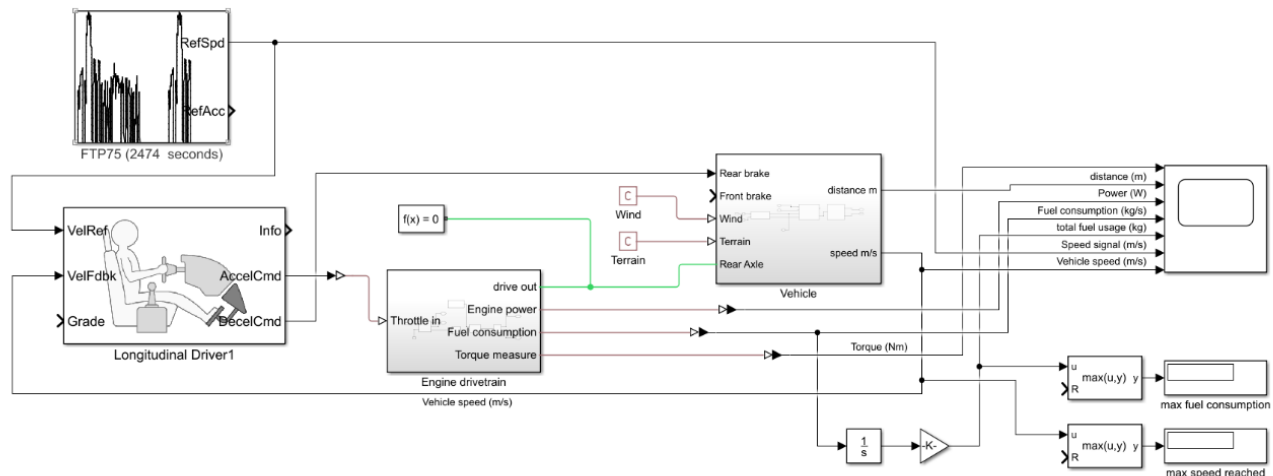


Figure 5: Model of the Vehicle showing the mechanical drivetrain

2.4 Detailed Drawing

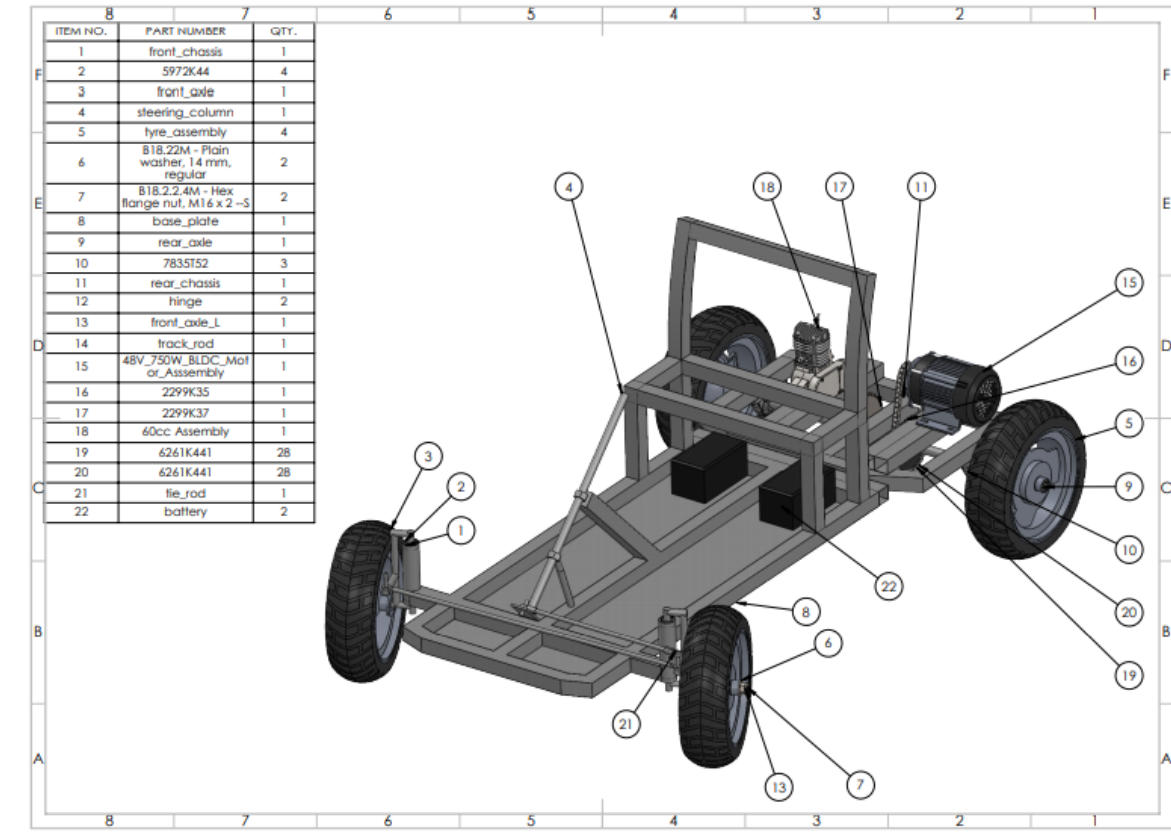


Figure 6: 3D model of the mini hybrid system showing its BOM

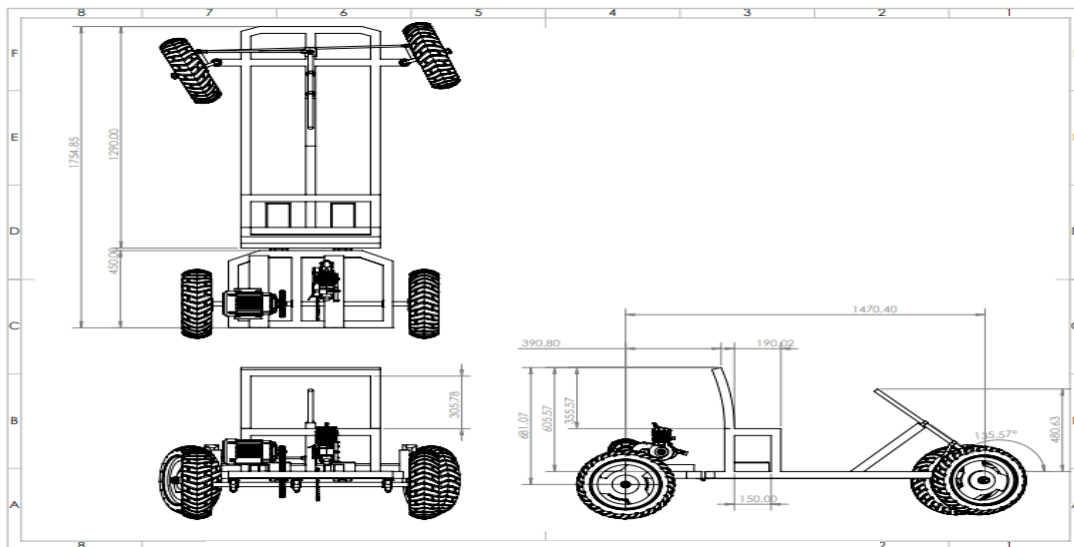


Figure 7: Detailed drawing of the mini hybrid electric vehicle

3.0. Results and Discussion

3.1 Static Analysis

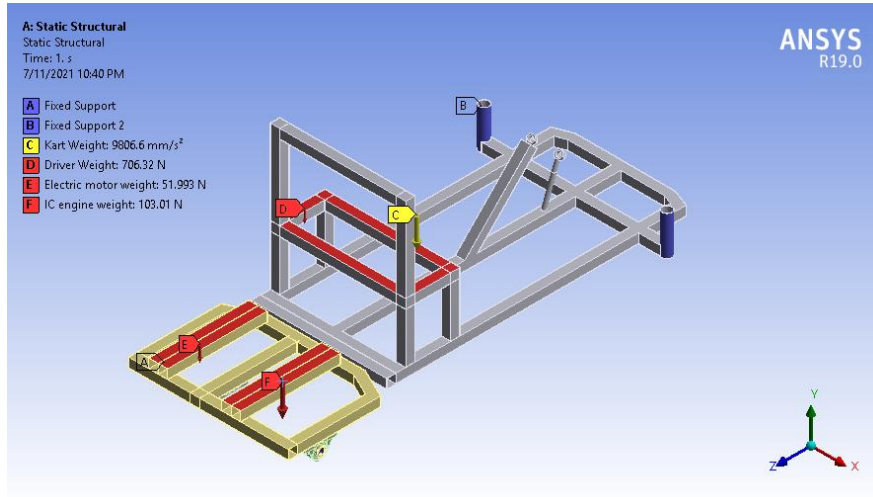


Figure 8: Constraints and loading for frame analysis

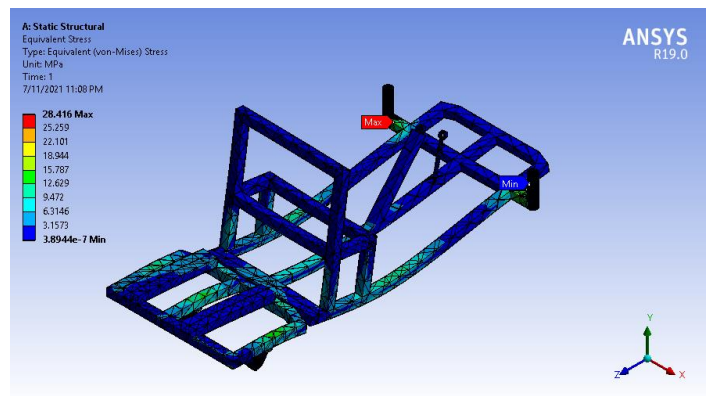
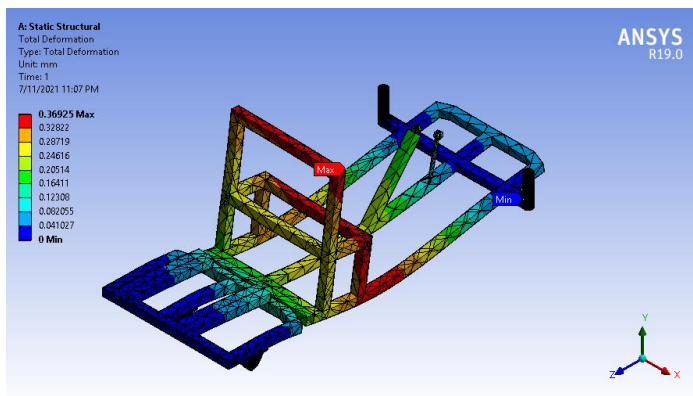


Figure 9: Total deformation and equivalent stress results for frame analysis



Figure 10: Constraints and loading for rear shaft analysis

Table 1: Summary of the simulated frame

| | |
|---------------------------|-----------|
| Maximum Deformation | 0.36925mm |
| Maximum equivalent stress | 28.416MPa |

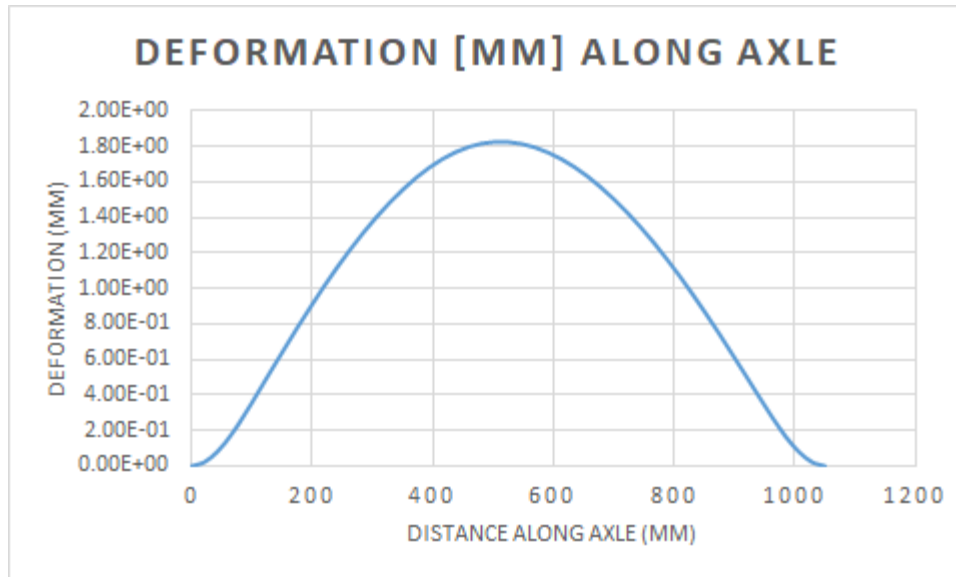


Figure 11: Graph of deformation along the rear shaft

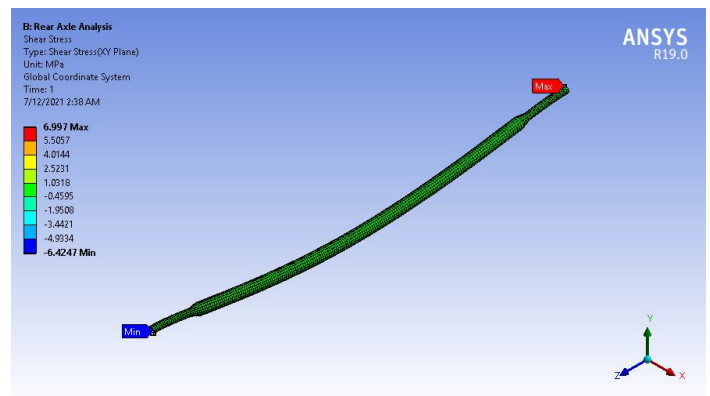
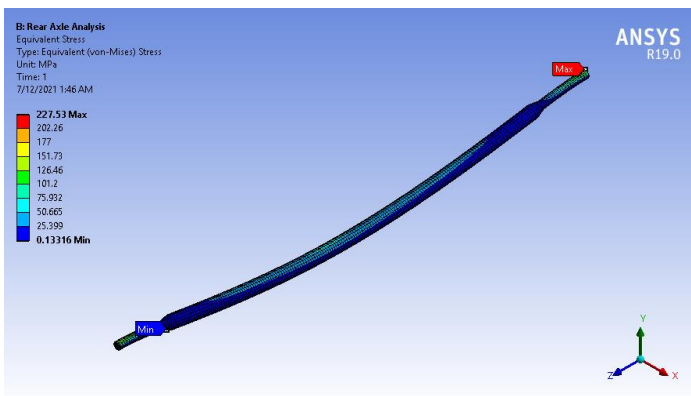


Figure 12: Equivalent stress and shear stress results for the rear shaft analysis

Table 2: Summary of simulation results for rear shaft analysis

| | |
|----------------------|-----------|
| Maximum deformation | 1.8256mm |
| Equivalent stress | 227.53MPa |
| Maximum shear stress | 6.997Mpa |

From Figure 11, maximum deformation occurs in the driver’s seat. Also, maximum Von Mises stress would occur in the front chassis close to the left housing for the front axle. It can also be seen that the maximum stress (28.4MPa) induced in the model didn’t exceed the yield stress for its material (370MPa). This implies that the chassis would be able to withstand the loads imposed on it.

From Figure 12, the maximum deformation occurs at the centre of the rear shaft. Also, the maximum equivalent and shear stresses induced in the shaft are less than the yield tensile stress (370MPa) and shear strength (80GPa) for mild steel. This maximum stress occurs at the corner of the shaft close to the IC engine. The reason for this is because the corner is a sharp edge that tends to build up stresses (has high-stress concentrations) when the model is subjected to a deforming load.

3.2 Dynamic Analysis

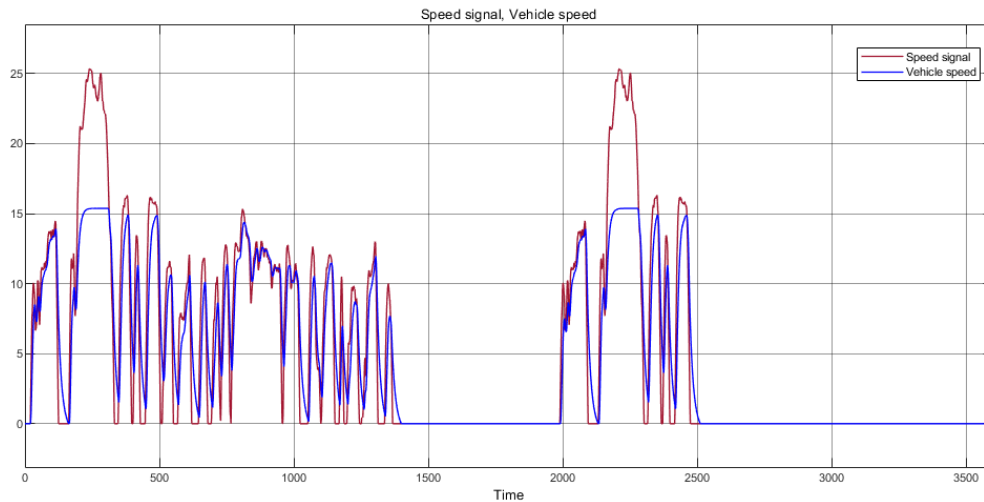


Figure 13: Reference and actual velocity (km/hr) of the vehicle based off the FTP75 drive cycle running on electric propulsion alone

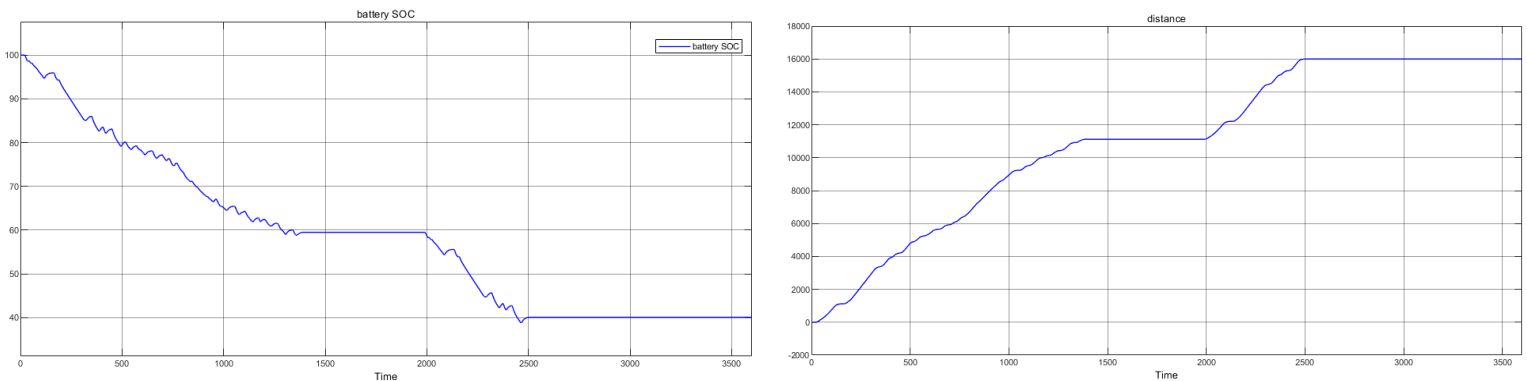


Figure 14: Graphs of battery SOC (%) and distance (m) against time for the hybrid system running on electric propulsion alone

Table 3: Summary of fuel consumption and max. speed for different IC engine

| Power (kW) | Max Speed (m/s) | Fuel Consumption ($\times 10^{-4}$ kg) |
|------------|-----------------|---|
| 0.75 | 14.35 | 3.5098 |
| 1.00 | 14.35 | 3.5098 |
| 1.50 | 14.35 | 4.0759 |
| 2.00 | 14.39 | 4.4342 |

| | | |
|-------------|--------------|---------------|
| 2.50 | 16.36 | 4.7019 |
| 3.00 | 18.05 | 4.907 |
| 3.50 | 19.52 | 5.060 |

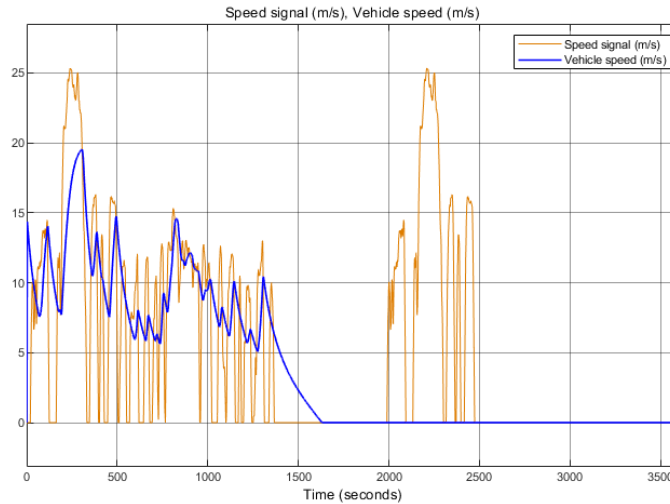


Figure 15: Reference and actual velocity response for the hybrid system running on the 3.5KW engine alone

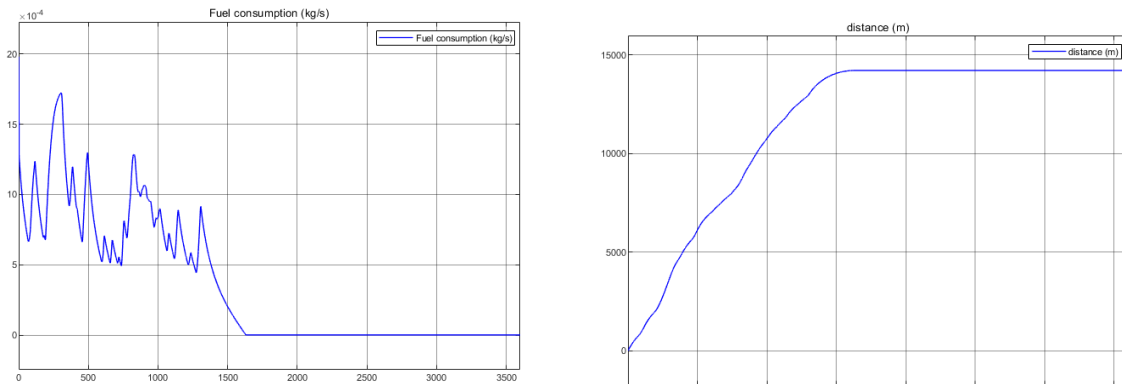


Figure 16: Graphs of fuel consumption (kg) and distance covered (m) vs time (s) for the hybrid system running on the 3.5KW engine alone

From Figure 14, the vehicle developed a top speed of **17km/hr** while running on electrical propulsion alone which is consistent with the preliminary analysis presented in section 2.2.1.2. Also, the vehicle covered 16000m during its motion while attaining a SOC of 40% at the end as shown in figure 15.

Table 3 shows the result from the analysis of the hybrid system running on IC propulsion alone for different engine power ratings. It can be seen that an engine with a rating of **3.5KW** would satisfy our requirements for the engine speed. The dynamic characteristics of the vehicle, when powered by this engine, is as shown in Figures 15 and 16.

3.3 System Analysis

From Equation1, the hybridization factor, HF, is given by

$$\text{Hybridization factor, HF} = \frac{\text{Motor power}}{\text{Motor power} + \text{Engine power}}$$

From the analysis presented above

Motor power = 0.75kW

Engine power = 3.5kW

$$\begin{aligned} HF &= \frac{0.75}{0.75 + 3.5} \\ &= 17.6\% \end{aligned}$$

$$\Rightarrow \text{Hybridization factor } HF = 17.6\%$$

Since the hybridization factor is greater than 10% but less than 30%, as shown in Table 1, the mini hybrid system is a **mild hybrid vehicle**.

4. Conclusion

A 3D representation of the mini hybrid system was created in Solidworks. Static and dynamic analysis of the computer model was carried out in Ansys and Simulink respectively and the results were presented in their respective sections.

Overall, it was found that the chassis and the rear shaft were stressed within acceptable limits. A **750W** BLDC motor was shown to be feasible for providing the low-speed torque with the vehicle reaching up to speeds of **17km/hr**. It was also shown that a **3.5kW** IC engine would be feasible for the high-speed requirements of the vehicle which was found to be **70km/hr**. The system was found to be a **mild hybrid vehicle** with a hybridization factor of **17.6%**.

4.1 Recommendations

1. The results from the simulation should be validated by building a physical model based on the specifications provided above and running it on a standard track with the FTP-75 as the reference drive cycle.
2. The fuel savings and overall efficiency of the hybrid should be determined and compared with that for the IC system working alone.
3. More complex systems like the series-parallel hybrid and the complex hybrid vehicles should be studied and compared with results from this study.
4. A stronger but lighter material other than mild steel should be investigated

Nomenclature

| | |
|-------|-------------------------------------|
| CAD | Computer-Aided Design |
| HEV | Hybrid Electric Vehicle |
| ZEV | Zero-Emission Vehicles |
| HC | Hydrocarbon |
| ICEV | Internal Combustion Engine Vehicles |
| ICE | Internal Combustion Engines |
| IC | Internal Combustion |
| HF | Hybridization Factor |
| SOC | State of Charge |
| AC | Alternating Current |
| DC | Direct Current |
| BLDC | Brushless DC |
| UDDS | Urban Dynamometer Driving Schedule |
| HWFET | Highway Fuel Economy Test |
| EM | Electric Motor |
| PWM | Pulse Width Modulation |

References

- [1] K. C. Prajapati, R. Patel, R. Sagar, B. T. Mechanical, and E. Student, "Hybrid Vehicle : A Study on Technology," *International Journal of Engineering Research & Technology (IJERT)*, vol. 3, no. 12, pp. 1076–1082, 2014.
- [2] N. Ha, "Comparative environmental impacts of Internal Combustion Engine Vehicles with Hybrid Vehicles and Electric Vehicles in China - Based on Life Cycle Assessment," *E3S Web of Conferences*, vol. 118, no. 2019, 2019, doi: 10.1051/e3sconf/201911802010.
- [3] C. C. Chan, "The State of the Art of Electric Vehicles," *Journal of Asian Electric Vehicles*, vol. 2, no. 2, pp. 579–600, 2004, doi: 10.4130/jaev.2.579.
- [4] A. Zia, "A comprehensive overview on the architecture of hybrid electric vehicles (hev)," in *2016 19th International Multi-Topic Conference (INMIC)*, 2016, pp. 1–7.
- [5] M. Kebriaei, A. H. Niasar, and B. Asaei, "Hybrid electric vehicles: An overview," in *2015 International Conference on Connected Vehicles and Expo (ICCVE)*, 2015, pp. 299–305. doi: 10.1109/ICCVE.2015.84.
- [6] N. Balasubramani, prasath S. Hari, K. A. Jagadeesh, P. S. Karna, and prasath D. Karun, "Fabrication and Performance Analysis of Hybrid Two Wheeler," *International Research Journal of Engineering and Technology (IRJET)*, vol. 5, no. 3, pp. 3672–3676, 2018.
- [7] E. Grunditz and E. Jansson, "Modelling and Simulation of a Hybrid Electric Vehicle for Shell Eco-marathon and an Electric Go-kart," *Power Engineering*, 2009.
- [8] K. Tammi, T. Minav, and J. Kortelainen, "Thirty years of electro-hybrid powertrain simulation," *IEEE access*, vol. 6, pp. 35250–35259, 2018.
- [9] S. M. Lukic and A. Emadi, "Effects of drivetrain hybridization on fuel economy and dynamic performance of parallel hybrid electric vehicles," *IEEE Transactions on Vehicular Technology*, vol. 53, no. 2, pp. 385–389, 2004, doi: 10.1109/TVT.2004.823525.
- [10] Collins C. Kwasi-Effah and Timon Rabczuk, "Dimensional Analysis and Modelling of a Lithium-Ion Battery. *Journal of Energy Storage*, Vol 18, pp308-315 2018, <https://doi.org/10.1016/j.est.2018.05.002>
- [11] Kwasi-Effah C.C, Obanor A.I "Simulation of the Emission Impact of a Hybrid-Electric Vehicle" *International Journal of Engineering & Technology Sciences (IJETS)* 1 (5): 251-259, 2013
- [12] C.C Kwasi-Effah, Al Obanor " Modeling and Simulation of a Gasoline-Electric Vehicle" *International Journal of Engineering & Technology*, 1(4) 163-176, 2013
- [13] CC Kwasi-Effah, Al Obanor, OO Ogbeide "Performance Investigation of a Series-Parallel Petrol-Electric Vehicle" *International Journal of Oil, Gas and Coal Engineering*, Vol 5(4): 54-60, 2017
- [14] M. Ceraolo, A. Di Donato, and G. Franceschi, "A general approach to energy optimization of hybrid electric vehicles," *IEEE Transactions on vehicular technology*, vol. 57, no. 3, pp. 1433–1441, 2008.
- [15] K. V Vidyanandan, "Overview of Electric and Hybrid Vehicles," 2018. [Online]. Available: <https://www.researchgate.net/publication/323497072>

Appendix

Table A1. Material properties for mild steel

| | | |
|---------------------------|---------------|-----------------------------------|
| Chemical composition | Carbon, C | 0.14 - 0.20% |
| | Iron, Fe | 98.81 – 99.26% |
| | Manganese, Mn | 0.60 – 0.90% |
| | Phosphorus, P | ≤ 0.040% |
| | Sulphur, S | ≤ 0.050% |
| Density | | $7.87 \times 10^5 \text{ kg/m}^3$ |
| Ultimate tensile strength | | 440Mpa |
| Yield tensile strength | | 370Mpa |
| Modulus of elasticity | | 205Gpa |
| Bulk modulus | | 140Gpa |
| Poisson ratio | | 0.290 |
| Shear modulus | | 80Gpa |